Hot and Cold Rolling of High Nitrogen Cr-Ni and Cr-Mn Austenitic Stainless Steels

R. Ilola, H. Hänninen, and T. Kauppi

(Submitted 8 April 1998; in revised form 27 May 1998)

Behavior of austenitic Cr-Ni-(0.14-0.50)N and Cr-Mn-(0.78-1.00)N steels in hot and cold rolling was investigated by rolling experiments and mechanical testing. Structure of the steels in the as-cast condition and fracture surfaces after the rolling experiments were investigated using optical and scanning electron microscopy (SEM). Resistance to deformation was calculated using rolling forces in hot rolling. Increase in strength in the rolling experiments was related to the nitrogen content of the steels. Resistance to deformation during hot rolling increased with decreasing rolling temperature and with increasing nitrogen content. In some steels, hot rolling led to edge cracking, which was more a function of impurity than nitrogen content. Microscopy revealed that the edge cracking occurred along grain boundaries and second phase particles. For the cold-rolled steels, the highest achievable reductions were limited due to a "crocodiling" phenomenon, that is, opening of the strip end. Fracture type at the opened strip end was a brittle-like fracture.

Keywords austenitic steels, forming, nitrogen steels, solution treatment, tensile properties

1. Introduction

Nitrogen has many beneficial effects on austenitic stainless steels. It stabilizes austenite by eliminating δ-ferrite formation at high temperatures and α′-martensite formation at low temperatures and during deformation. Nitrogen increases the yield strength of austenite more than other alloying elements, and it also improves corrosion, stress corrosion, and creep resistance of austenitic stainless steels (Ref 1). Hot and cold workability are of great importance when austenitic high nitrogen steels are manufactured for industrial applications, where the combination of high strength and toughness, nonmagnetism, and good corrosion properties are typically required. These applications are, for example, oil exploration equipment, wear resistant parts in electronic equipment, and generator retaining rings (Ref 2, 3).

The aim of this study was to investigate formability, tendency to cracking, resistance to deformation, achievable reductions, and other deformation limiting factors of austenitic high nitrogen steels.

2. Experimental Procedure

The test materials were nitrogen alloyed (0.14 to 1.00 wt% N) chromium-nickel and chromium-manganese type austenitic stainless steels. Table 1 presents compositions of the test materials. All test materials were laboratory scale heats. Test material ingots of 50 kg in mass were melted in an open arc furnace and remelted under elevated nitrogen pressure using a plasma arc method for addition of nitrogen. The plasma arc remelted ingots were made in the Izevsk Steel Plant in Russia.

Remelted ingots were hot rolled at Outokumpu Polarit Oy (Tornio, Finland) with a pilot scale rolling mill. The diameter of the work rolls was 450 mm for hot rolling. Prior to the hot rolling, the ingots of 68 by 68 mm^2 in size were heated to 1250 °C and then hot rolled down to approximately 950 °C. The pass schedule was the same for all steels, and target thicknesses per pass were 50, 37, 27, 21, 17, 14, 11, and 8 mm. Hot-rolling parameters (force, moment, etc.) were detected using a computer-based data acquisition system during the experiments.

Resistance to deformation during hot rolling was calculated from the measured rolling forces using Eq 1 (Ref 4):

$$\frac{P}{\bar{k}} = L\left(1.571 + \frac{L}{h_1 + h_2}\right) \quad \text{(Eq 1)}$$

where P is rolling force per unit width, L is length of arc of contact of the roll, h_1 is strip thickness at entry to the pass, h_2 is strip thickness at exit from the pass, and $\bar{k}$ is mean shear yield stress in the pass.

The length of arc of contact (L) is:

$$L = \sqrt{R(h_1 - h_2)} \quad \text{(Eq 2)}$$

where R is radius of the roll.

After the hot-rolling experiments, the amount of edge cracking was determined visually.

The 19Cr-8Ni-0.26N, 19Cr-8Ni-0.50N, 19Cr-15Mn-0.80N, and 22Cr-12Mn-1.00N steels were also studied in the solution annealed condition. Solution annealing temperatures varied for each steel, from 1085 to 1280 °C, and they were selected to prevent Cr_2N formation during the annealing (Ref 5).

Cold rolling was performed on 19Cr-8Ni-0.50N and 22Cr-12Mn-1.00N steels in a hot-rolled condition. The diameter of

R. Ilola and **H. Hänninen,** Helsinki University of Technology, Laboratory of Engineering Materials, P.O. Box 4200, FIN-02015 HUT, Finland; and **T. Kauppi,** Outokumpu Polarit Oy, FIN-95400 Tornio, Finland.

the work rolls used in cold rolling was 135 mm. The goal of the cold-rolling experiments was to study the maximum achievable reduction values of the steels.

Mechanical properties of the studied steels were determined using tensile tests and hardness measurements. Hardness was measured from all steels in the as-cast and hot-rolled conditions using Vickers (10 HV) and Brinell methods, respectively. The Brinell hardness values were then converted to Vickers values. Tensile tests were performed on 19Cr-8Ni-0.26N, 19Cr-8Ni-0.50N, 19Cr-15Mn-0.80N, and 22Cr-12Mn-1.00N steels in the hot-rolled and solution annealed conditions. Proportional test specimens with a diameter of 5 mm were used in the tests. 19Cr-8Ni-0.50N and 22Cr-12Mn-1.00N steels were also tested in the cold-rolled condition using flat tensile specimens of 12 mm in width and 110 mm in gauge length. The specimen thickness was the sheet thickness after cold rolling. Yield strength, tensile strength, and elongation values were determined in the tests.

Structure of the test materials and possible fracture surfaces after the rolling experiments were characterized using optical and scanning electron microscopy (SEM).

Austenite stability against α'-martensite formation during the cold rolling experiments was measured by means of magnetic measurements using a Feritscope MP3C ferrite gauge (Fischer Technology, Inc., Windsor, CT). The measurements

Table 1 Chemical compositions of the test materials (wt%)

Steel	C	Si	Mn	Cr	Ni	Mo	Nb	V	W	N
19Cr-9Ni-0.14N	0.020	0.27	0.17	18.9	8.5	0.04	0.32	<0.01	0.01	0.137
18Cr-9Ni-0.20N	0.013	0.24	0.19	17.5	8.5	0.08	<0.01	<0.01	<0.01	0.197
18Cr-9Ni-0.22N	0.011	0.24	0.15	18.0	8.6	0.04	<0.01	<0.01	0.01	0.220
19Cr-8Ni-0.26N	0.009	0.23	0.09	18.8	7.7	<0.01	<0.01	0.12	<0.01	0.264
19Cr-9Ni-0.45N	0.017	0.26	0.14	18.7	8.5	0.04	0.30	<0.01	0.01	0.450
19Cr-8Ni-0.50N	0.009	0.25	0.09	18.8	7.7	<0.01	<0.01	0.12	0.01	0.500
19Cr-15Mn-0.78N	0.016	0.07	15.00	19.0	0.2	0.02	<0.01	0.01	0.05	0.780
19Cr-15Mn-0.80N	0.018	0.07	15.17	18.9	0.2	0.02	<0.01	0.01	0.05	0.800
22Cr-12Mn-0.97N	0.017	0.10	12.30	22.2	0.4	0.03	<0.01	0.01	0.02	0.970
22Cr-12Mn-1.00N	0.017	0.11	12.20	22.1	0.4	0.03	<0.01	0.01	0.02	0.100

Table 2 Amount of edge cracking together with the impurity contents of various high-nitrogen, austenitic stainless steels

		Impurity content, wt%				
	Steel	S	P	Cu	Sn	O
Small	18Cr-9Ni-0.22N	0.007	0.002	<0.01	<0.002	(a)
	19Cr-9Ni-0.14N	0.006	0.005	0.12	0.003	(a)
	22Cr-12Mn-1.00N	0.008	0.007	0.02	0.010	0.011
	18Cr-9Ni-0.20N	0.006	0.002	0.01	<0.002	(a)
	19Cr-8Ni-0.26N	0.006	<0.002	0.01	0.002	0.011
	22Cr-12Mn-0.97N	0.009	0.005	0.01	0.012	(a)
Large	19Cr-8Ni-0.50N	0.004	0.002	0.01	<0.002	0.022
	19Cr-15Mn-0.78N	0.011	0.006	2.10	0.013	(a)
	19Cr-9Ni-0.45N	0.006	0.006	0.11	0.002	0.019
	19Cr-15Mn-0.80N	0.006	0.007	2.05	0.010	0.011

(a) Not measured

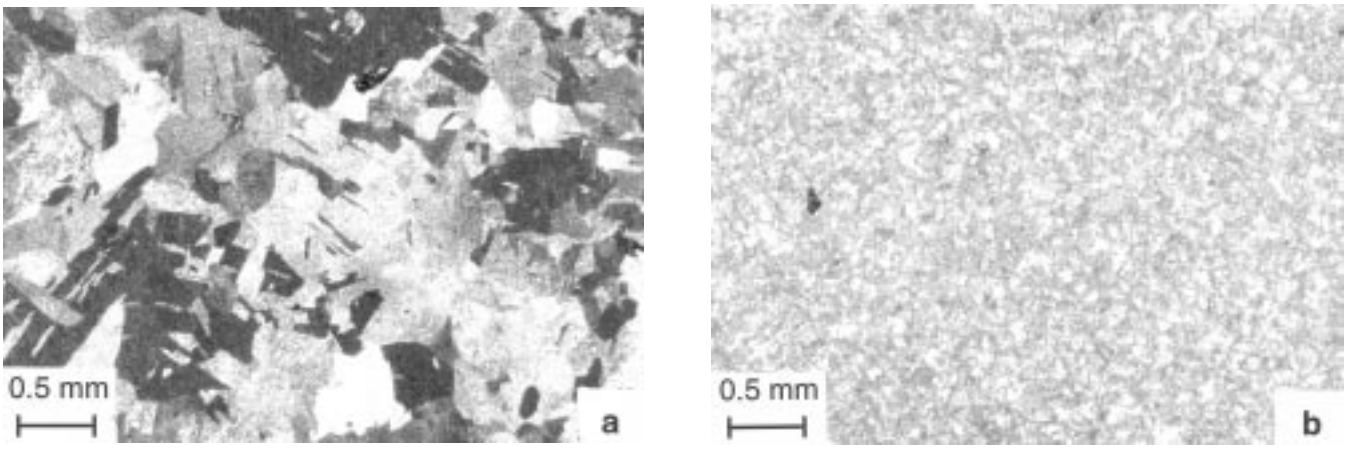

Fig. 1 Macrographs taken from the middle of the cross sections of remelted ingots. (a) 19Cr-8Ni-0.26N steel. (b) 22Cr-12Mn-0.97N steel

were done from several points from the rolled surface after which an average α′-martensite content was calculated.

3. Results and Discussion

3.1 As-Cast Condition

Macrographs of the cross sections of the remelted ingots revealed that the grain size varied in large ranges between the different alloys and also within the cross sections (Fig. 1a, b). No systematic correlations between the microstructures and the alloy compositions were observed. However, the grain size of the chromium-nickel steel ingots seemed to be larger, and its variation within the cross section was greater than that in the chromium-manganese steel ingots. A common observation was that the grain size was the largest in the middle of the cross section, and the grains were mainly equiaxed.

3.2 Hot Rolling Experiments and Solution Annealing

Resistance to deformation logarithmic regression curves are presented in Fig. 2 and 3 for the studied high nitrogen chromium-nickel and chromium-manganese steels, respectively. With both types of steels studied, resistance to deformation increased with decreasing rolling temperature and with increasing nitrogen content. However, some scatter occurred in the results. Resistance to deformation values of chromium-nickel type steels with 0.45 and 0.50 wt% N was at the same level as those of 19Cr-15Mn steels with 0.78 and 0.80 wt% N. The highest resistance to deformation values was observed with 22Cr-12Mn steels (0.97 and 1.00 wt% N).

Edge Cracking. Table 2 presents the tendency for edge cracking during the hot rolling experiments, from the best steel to the worst. Edge cracking was minor in 18Cr-9Ni-0.22N, 19Cr-9Ni-0.14N, 22Cr-12Mn-1.00N, 18Cr-9Ni-0.20N, 19Cr-8Ni-0.26N, and 22Cr-12Mn-0.97N steels. Practically no edge cracking was observed in 18Cr-9Ni-0.22N steel. In 19Cr-8Ni-0.50N, 19Cr-15Mn-0.78N, 19Cr-9Ni-0.45N, and 19Cr-15Mn-0.80N steels the cracks were large, and they were clearly visible on the surfaces of the hot-rolled samples. In the 19Cr-15Mn-0.80N steel the depth of the cracks was over 10 mm.

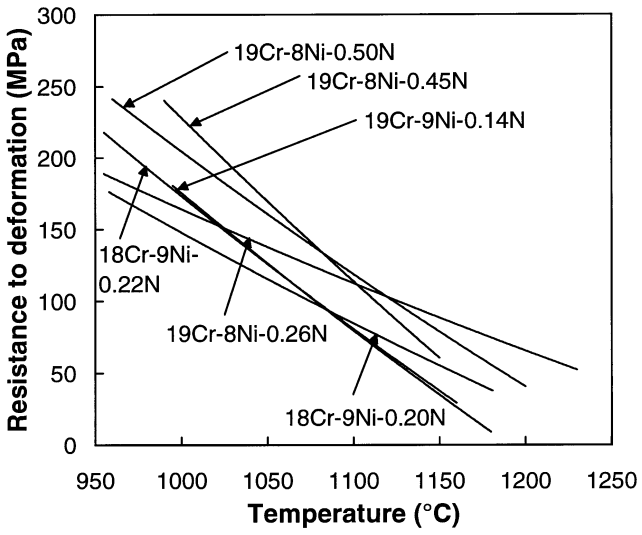

Fig. 2 Resistance to deformation logarithmic regression curves of high-nitrogen, chromium-nickel steels during hot rolling as a function of temperature

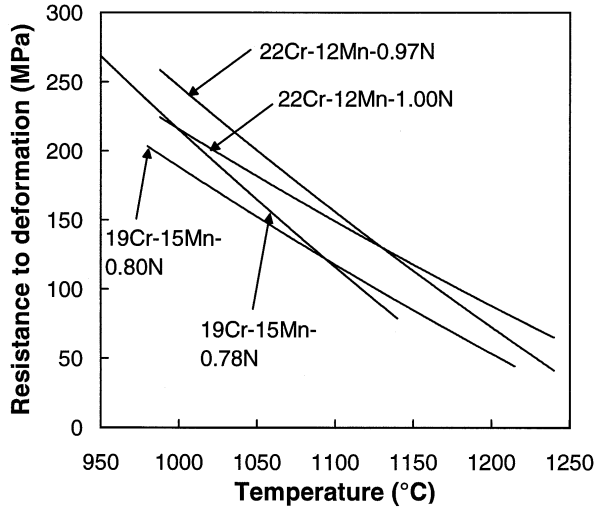

Fig. 3 Resistance to deformation logarithmic regression curves of high-nitrogen, chromium-manganese steels during hot rolling as a function of temperature

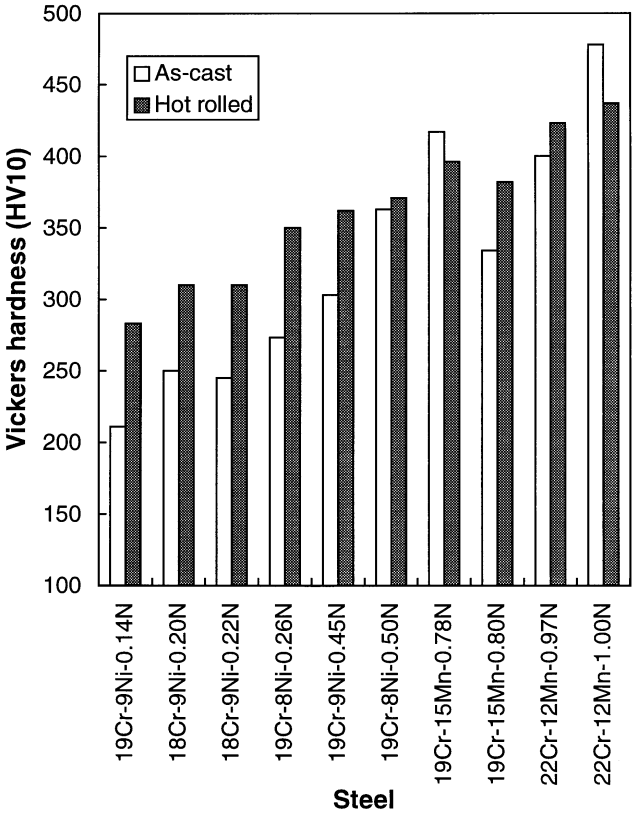

Fig. 4 Comparison of hardness (10 HV) between remelted ingots (as-cast) and hot-rolled conditions of chromium-nickel and chromium-manganese type high-nitrogen steels

Tendency to edge cracking was not a function of nitrogen content, strength, or resistance to deformation in the investigation. No systematic difference in edge cracking was found between the studied chromium-nickel and chromium-manganese steels. However, some correlation between the amount of edge cracking and impurity content was observed. In the steels showing most of edge cracking, either sulfur, phosphorus, copper, tin, or oxygen content or their combination was relatively higher than for the other compositions. Detrimental effects of sulfur and oxygen contents on hot workability of high-nitrogen, austenitic stainless steels have also been previously observed (Ref 6).

Mechanical Properties. Figure 4 presents hardness values of the hot-rolled steels together with the remelted ingots. It shows clearly the austenite solid solution strengthening effect of nitrogen. Hot rolling increased strength as compared to the as-cast condition. Hardness values of the studied steels in the hot-rolled condition indicate tensile strength values from 980 to 1200 MPa for chromium-nickel steels (0.20 to 0.50 wt% N) and from 1200 to 1400 MPa for chromium-manganese steels (0.78 to 1.00 wt% N). Increasing the effect of hot rolling on hardness was the greatest with low nitrogen contents of chromium-nickel steels. In two cases the hardness of the remelted ingots was higher than that of the hot-rolled condition (19Cr-15Mn-0.78N and 22Cr-12Mn-1.00N steels). Commonly, the hardness of the chromium-manganese steels was greater than that of the chromium-nickel steels because of the higher nitrogen contents of the chromium-nickel steels. Also, the strengthening effect of manganese on austenite is greater as compared to that of nickel (Ref 1).

Figure 5 presents tensile test results in the hot-rolled and solution annealed conditions. Yield strength in the hot-rolled condition was roughly twice as much as that in the solution annealed condition, and the largest difference between these two conditions occurred with 19Cr-8Ni-0.50N steel, being approximately 590 MPa. With 22Cr-12Mn-1.00N steel, a yield strength value of approximately 1200 MPa was measured in the hot-rolled condition. As the yield strength decreased during the solution annealing, the elongation values were roughly doubled (from approximately 30 to approximately 60%). Tensile properties of the tested chromium-nickel steels in the solution annealed condition were in accordance with the literature data and resembled the behavior of AISI 304 type austenitic stainless steel (Ref 7). Decrease in the tensile strength during solution annealing was much smaller than in the yield strength for both types of steels, and steel type or nitrogen content had only a small influence on it.

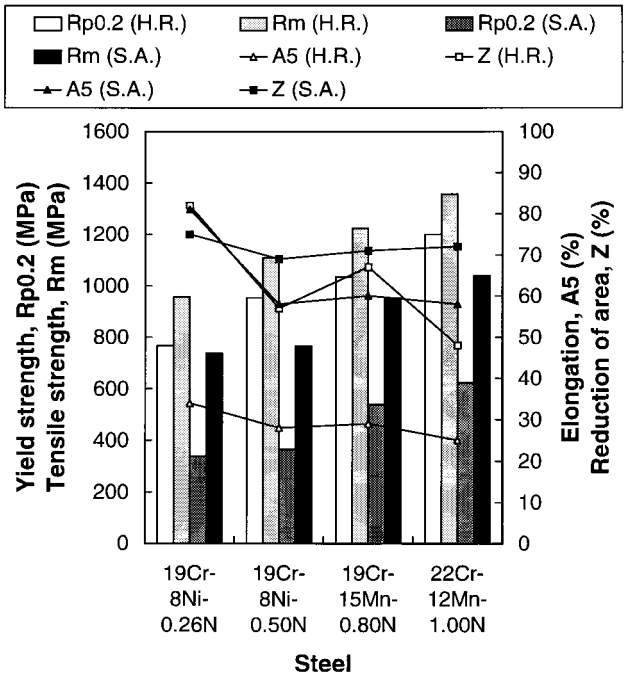

Fig. 5 Tensile properties of hot-rolled (H.R.) and solution annealed (S.A.) chromium-nickel and chromium-manganese type austenitic high-nitrogen steels

Microscopy. Scanning electron microscopy and optical microscopy showed that the fracture path of edge cracking during hot rolling followed austenite grain boundaries (Fig. 6) and second phase particles (Fig. 7). According to energy dispersive x-ray (EDX) point analysis, these particles were iron, chromium, and nickel containing oxides in the severely edge-cracked, chromium-nickel steels. In the severely edge-cracked, chromium-manganese steels, the second phase particles also contained copper and tin (0.78 and 0.80N steels). These elements may have led to formation of a low melting point phase, which caused the edge cracking in these steels. From solution annealed 0.78N and 0.80N steels, copper and tin containing particles were also found on grain boundaries (Fig. 8) and within the grains (Fig. 9). However, steel structure was not uniform through the studied samples. Figure 10 presents a fractograph taken from an edge-cracked area of 19Cr-15Mn-0.80N steel showing ductile fracture.

According to Ref 1, segregation of nitrogen, and especially chromium-nickel clusters, on austenite grain boundaries also reduce hot ductility by retarding recovery and recrystallization of austenite. Detrimental effect of Cr_2N precipitates on hot workability was also reported by Mineura and Tanaka (Ref 6). These precipitates were not found on the austenite grain boundaries by EDX analysis in this investigation, but their presence cannot be excluded because the hot-rolling experiments were performed in the temperature range where the precipitation occurs.

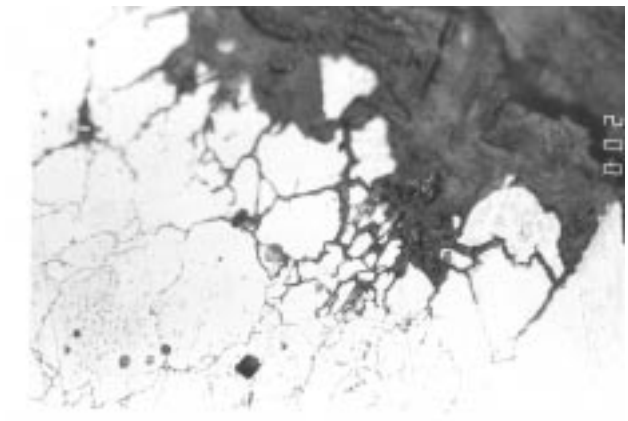

Fig. 6 Crack propagation along austenite grain boundaries during hot rolling in 19Cr-8Ni-0.50N steel

3.3 Cold-Rolling Experiments

Cold-rolling experiments were performed with 19Cr-8Ni-0.50N and 22Cr-12Mn-1.00N steels. With 0.50N steel, the highest reduction achieved was 56%. After this, cold rolling was limited by a "crocodiling" phenomenon, that is, opening of the strip end, and cold rolling could not be continued any further. With 1.00N steel, the highest reduction achieved was 7%. Nitrogen alloyed austenitic steels exhibit high-work hardening rate, which controls their formability (Ref 1).

Mechanical Properties. Tensile test results of cold rolled 19Cr-8Ni-0.50N and 22Cr-12Mn-1.00N steels are presented in Fig. 11. Twenty percent cold rolling of 19Cr-8Ni-0.50N steel (after hot rolling) increased the yield strength up to 1170 MPa, and further cold rolling, up to 56%, increased the yield strength to approximately 1430 MPa. The corresponding decrease in the elongation values was from 24 to 7%. 22Cr-12Mn-1.00N steel in 7% cold-rolled condition exhibited yield and tensile strength values of 1200 and 1450 MPa, respectively. The corresponding tensile elongation value was 15% (Fig. 11).

Microscopy. Figure 12 shows the fracture surface of the "crocodiled" area in 7% cold rolled 22Cr-12Mn-1.00N steel. The fracture surface has features of both ductile dimpled and transgranular brittle-like fracture and thus, it is considered a quasi-cleavage fracture. Transgranular fracture has also been observed in these steels during deformation at low temperatures (Ref 8).

Austenite Stability. All steels were fully austenitic after the hot-rolling experiments according to the magnetic measurements, but 56% cold rolling of 19Cr-8Ni-0.50N steel produced

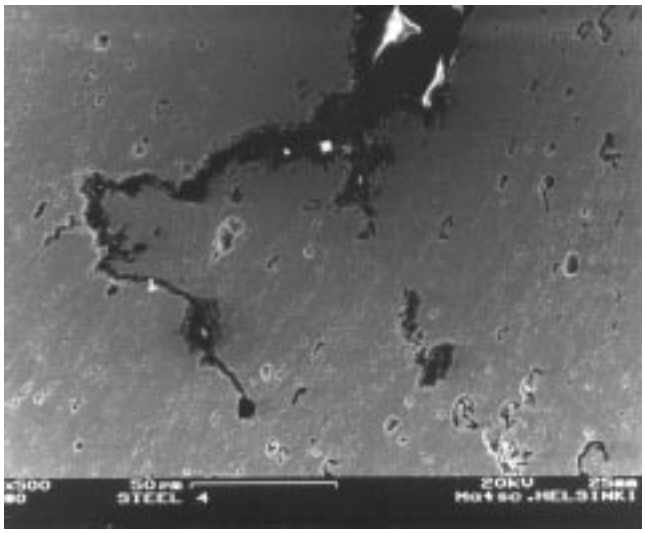

Fig. 7 Crack propagation along second phase particles during hot rolling in 19Cr-8Ni-0.50N steel. (Art has been reduced to 77% of its original size for printing.)

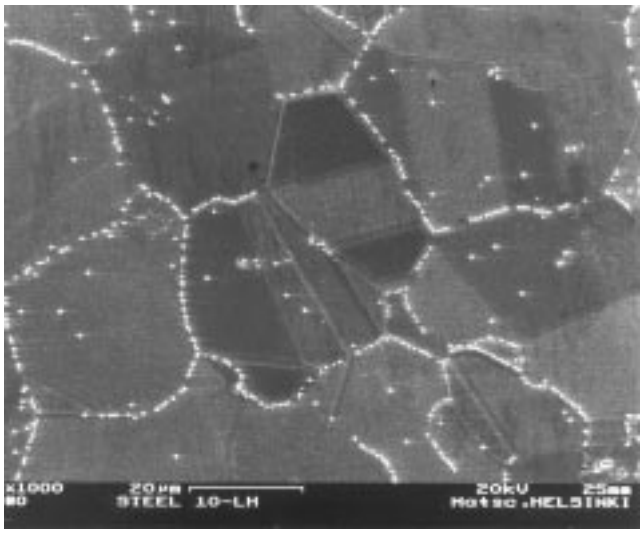

Fig. 8 Copper- and tin-containing particles on grain boundaries in solution annealed 19Cr-15Mn-0.80N steel. (Art has been reduced to 77% of its original size for printing.)

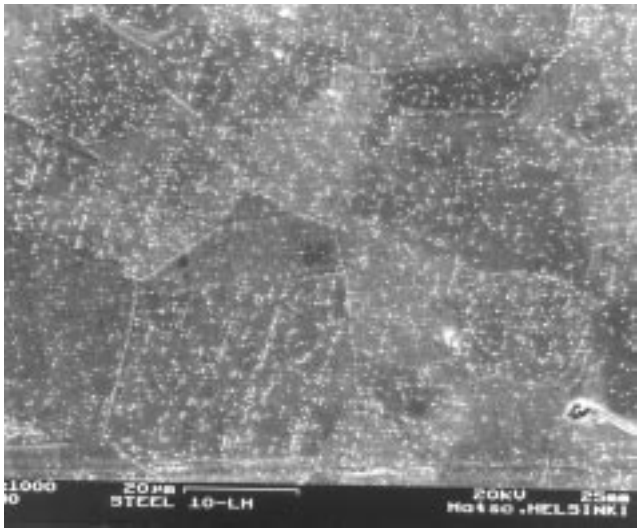

Fig. 9 Copper- and tin-containing particles within grains in solution annealed 19Cr-15Mn-0.80N steel. (Art has been reduced to 77% of its original size for printing.)

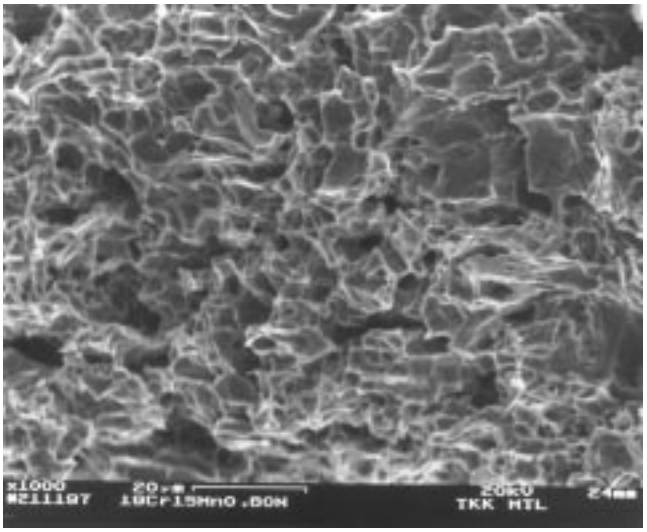

Fig. 10 Ductile fracture surface from an edge-cracked area of 19Cr-15Mn-0.80N steel. (Art has been reduced to 77% of its original size for printing.)

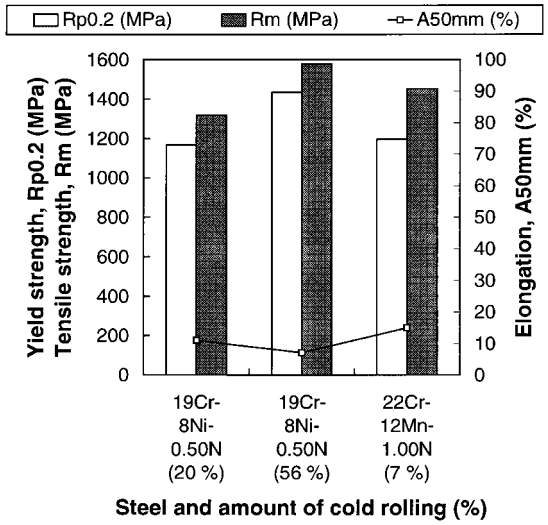

Fig. 11 Tensile properties of cold-rolled 19Cr-8Ni-0.50N and 22Cr-12Mn-1.00N steels

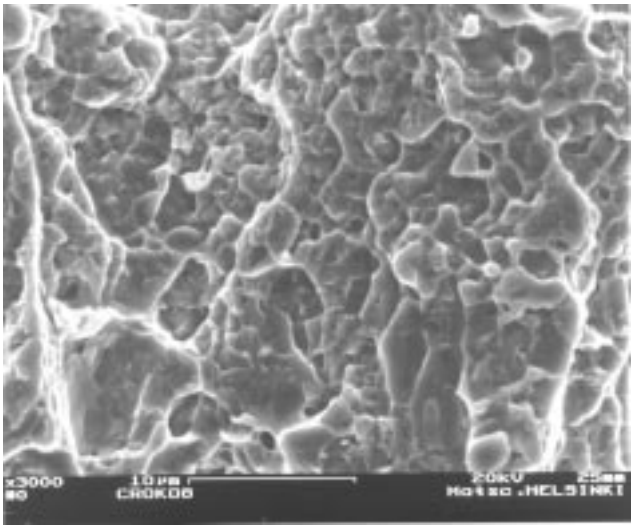

Fig. 12 Fractograph taken from a "crocodiled" fracture surface of 7% cold-rolled 22Cr-12Mn-1.00N steel. (Art has been reduced to 77% of its original size for printing.)

approximately 4% ferromagnetic phase, that is, α′-martensite. For the 20% cold-rolled sample, the measured content was approximately 1%. Thus, 0.50 wt% N content was not adequate for preventing α′-martensite formation entirely in 19Cr-8Ni type austenitic stainless steels. No α′-martensite was measured from the cold rolled 22Cr-12Mn-1.00N steel.

4. Conclusions

Formability of austenitic high nitrogen chromium-nickel and chromium-manganese steels was investigated using hot- and cold-rolling experiments. Mechanical properties were studied in solution annealed and hot- and cold-rolled conditions. This investigation led to following conclusions. Strength of the studied steels was superior after hot rolling as compared to the as-cast or solution annealed conditions, and it was clearly related to the nitrogen content of the steels. Resistance to deformation during hot rolling increased with decreasing rolling temperature and with increasing nitrogen content. Amount of edge cracking, which occurred along grain boundaries and second phase particles during hot rolling, was mainly a function of the impurity and not the nitrogen content. For the two cold-rolled steels, the highest achievable reductions were limited due to a "crocodiling" phenomenon, that is, opening of the strip end. Fracture surface at the strip end consisted of a quasi-cleavage type fracture.

References

1. F.B. Pickering, Some Beneficial Effects of Nitrogen in Steel, *Proc. of the Int. Conf. on High Nitrogen Steels HNS 88*, J. Foct and A. Hendry, Ed., The Institute of Metals, London, 1989, p 10-31
2. M.O. Speidel, Properties and Applications of High Nitrogen Steels, *Proc. of the Int. Conf. on High Nitrogen Steels HNS 88*, J. Foct and A. Hendry, Ed., The Institute of Metals, London, 1989, p 92-96
3. G. Stein and J. Lueg, High Nitrogen Steels—Applications in Present and Future, *Proc. of the 3rd Int. Conf. on High Nitrogen Steels HNS 93*, V.G. Gavriljuk and V.M. Nadutov, Ed., Institute for Metal Physics, Kiev, 1993, p 31-37
4. H. Ford and J.M. Alexander, Simplified Hot-Rolling Calculations, *J. Institute Met.*, Vol 92 (No. 1963-64), 1964, p 397-404
5. X. Zheng, *Nitrogen Solubility in Iron-Base Alloys and Powder Metallurgy of High Nitrogen Steels*, Swiss Federal Institute of Technology, Zürich, 1991, p 110
6. K. Mineura and K. Tanaka, Effect of Calcium Treatment on Hot Workability of Cr-Ni-0.7N Stainless Steel, *Mater. Sci. Technol.*, Vol 6 (No. 8), 1990, p 743-748
7. R.P. Reed, Nitrogen in Austenitic Stainless Steels, *JOM*, Vol 41 (No. 3), 1989, p 16-21
8. R.J. Ilola, H.E. Hänninen, and K.M. Ullakko, Mechanical Properties of Austenitic High-Nitrogen Cr-Ni and Cr-Mn Steels at Low Temperatures, *ISIJ Int.*, Vol 36 (No. 7), 1996, p 873-877